Cu-Al2O3 Water Hybrid Nanofluid Transport in a Periodic Structure

Authors:

Aiman Alshare, Wael Al-Kouz, Waqar Khan

Date Submitted: 2020-05-08

Keywords: heat transfer augmentation, hybrid nanofluid, nanofluid, periodic, Cu-Al2O3, wavy channel

Abstract:

The present work is a computational investigation of nanofluid and hybrid nanofluid transport in a periodic structure. The governing equations for this work along with the appropriate boundary conditions are solved using the finite-volume method. The simulations are carried out using five wavy amplitudes of the channel shape for a range of Reynolds numbers from 102 to103. It is found that increasing the amplitude and increasing the nanoparticle volume fraction achieve enhancement of the heat transfer at the cost of increased pumping power. Correlations for the friction factor and the Nusselt number for both fluid types are provided.

Record Type: Published Article

Submitted To: LAPSE (Living Archive for Process Systems Engineering)

Citation (overall record, always the latest version):	LAPSE:2020.0430
Citation (this specific file, latest version):	LAPSE:2020.0430-1
Citation (this specific file, this version):	LAPSE:2020.0430-1v1

DOI of Published Version: https://doi.org/10.3390/pr8030285

processes

MDPI

Article

Cu-Al_2O_3 Water Hybrid Nanofluid Transport in a Periodic Structure

Aiman Alshare [1,*], Wael Al-Kouz [1] and Waqar Khan [2]

[1] Mechatronics Engineering Department, German Jordanian University, Amman 11180, Jordan; wael.alkouz@gju.edu.jo

[2] Mechanical Engineering Department, Prince Mohammad Bin Fahd University, Al-Khobar 31952, Saudi Arabia; WKHAN@pmu.edu.sa

* Correspondence: aiman.share@gju.edu.jo

Received: 22 December 2019; Accepted: 24 February 2020; Published: 3 March 2020

Abstract: The present work is a computational investigation of nanofluid and hybrid nanofluid transport in a periodic structure. The governing equations for this work along with the appropriate boundary conditions are solved using the finite-volume method. The simulations are carried out using five wavy amplitudes of the channel shape for a range of Reynolds numbers from 10^2 to10^3. It is found that increasing the amplitude and increasing the nanoparticle volume fraction achieve enhancement of the heat transfer at the cost of increased pumping power. Correlations for the friction factor and the Nusselt number for both fluid types are provided.

Keywords: wavy channel; Cu-Al_2O_3; periodic; nanofluid; hybrid nanofluid; heat transfer augmentation

1. Introduction

In several engineering applications, microelectronics and compact heat exchangers need significant enhancement in heat transfer. The use of fins, cavities, wavy surfaces, channels or nanofluids can provide substantial heat transfer enhancement in these applications. In case of heat exchangers, nanofluids in the wavy channels offer a much better heat transfer rate. In their review, Hussien et al. [1] summarized some brief survey methods to prepare hybrid nanofluids along with their superior thermal properties compared to base fluids. Several numerical studies, related to the fully developed flows in periodic geometries, exist in the literature [2–8]. Sarkar et al. [9] considered a furrowed wavy channel at various Reynolds numbers and noticed that critical Reynolds number decreases with an increase in the amplitude and wavelength. They demonstrated that with increasing Reynolds number, Nusselt number, friction, area-goodness, and thermal-performance factors remain unchanged in the steady regime and grow almost linearly in the unsteady regime. Bahaidarah et al. [10–12] considered wavy channels with sinusoidal and arc-shaped configurations and compared their numerical results with a parallel-plate channel. They found a negligible increase in heat transfer at low Reynolds number for the two selected configurations as compared to the straight channel. However, at higher Reynolds number, up to 80%, high heat transfer rates were observed. Xie et al. [13] considered a wavy channel and studied the effects of amplitude, lengths, channel widths, and longitudinal pitches on the fluid flow and heat transfer in the channel. They demonstrated that the friction factors and the overall Nusselt numbers rise with an increase in the channel width and Reynold numbers.

Besides these numerical studies, there are also several experimental studies on the fluid flow and heat transfer in periodic channels. A few of them will be summarized here. Rush et al. [14] investigated the flow and local heat transfer rates experimentally for laminar and transitional regimes in wavy passages. They found a substantial increase in the local heat transfer with an increase in the Reynolds

number. In series of papers, Nishimura and co-workers [15–20] experimentally investigated the steady flow, heat, and mass transfer features in wavy channels, including the sine-shaped and arc-shaped, at moderate Reynolds number. It was noticed that, for a steady flow, the mass transfer rates were negligible whereas the mass transfer rates were high when the flow became unsteady. They presented the variation of friction and pressure drop with the Reynolds number. They demonstrated that the reversed-flow region significantly differs from the forward-flow region with the help of local Sherwood number distributions. For the arc-shaped wall, a new flow structure was observed at a low Reynolds number. When flow separation occurs, the mass transfer features of both channels differ from each other. The mass transfer rate was found to be higher for the arc-shaped channel.

It is important to note that conventional fluids were used in all the above studies. It has been proved experimentally and numerically that nanofluids can be used in various geometries to enhance heat transfer rates [21–30]. Using different nanofluids, Yang et al. [31] enhanced the heat transfer rate in a wavy channel and validated their numerical results with the existing literature. They optimized their results by using a full factorial experimental design and the genetic algorithm (GA) method. Rashidi et al. [32] employed both single- and two-phase models of nanofluids in a wavy channel and investigated the flow and heat transfer. They noted enhancement in the heat transfer with an increase in the volume fraction of nanoparticles and Reynolds number. Akdag et al. [33] demonstrated that, in wavy channels, thermal performance could be enhanced significantly by using nanoparticles under pulsating conditions. Using Buongiorno's mathematical model, Shehzad et al. [34] examined the effects of convective heat transfer of nanofluids in a wavy channel. They concluded that Nusselt and Sherwood numbers depend upon the Prandtl number of the nanofluid in the channel.

Albojamal et al. [35] studied the effects of pertinent parameters on the flow and heat transfer of nanofluids in a wavy channel. They noticed that the nanofluids with variable properties enhance heat transfer rates significantly. They also confirmed an increase in heat transfer with increasing Reynolds number and the solid volume fraction of nanoparticles at the cost of higher pressure drop. Ahmed et al. [36] investigated the effects of governing parameters on the flow and heat transfer of a nanofluid in a wavy channel. Their results reveal an increase in the friction and heat transfer rate with an increase in the solid volume fraction of nanoparticles, Reynolds number, and the amplitude of the wavy channel. Moreover, Hader et al. [37] investigated the performance of a hybrid photovoltaic/thermal system by utilizing Al_2O_3 nanofluid; they found that dispersing solid particles in the base fluid will enhance the heat transfer and consequently will improve the overall efficiency of such systems. Bozorg et al. [38] employed a porous fin and synthetic oil-Al_2O_3 in a parabolic trough solar receiver system. They found that the thermal and overall efficiency of the system increase linearly with Reynolds number, whilst the inclusion of the porous fin increases the required pumping power.

Periodically fully developed hybrid nanofluid flow in a wavy channel can potentially be an asset for a host of industrial applications where compact design combined with an efficient rate of heat removal is required, which could result in savings of material, weight, and cost. Therefore, the focus of this paper is to study hydrodynamically and thermally periodically fully developed flow and heat transfer of Cu–Al_2O_3 water-based hybrid nanofluid in a wavy channel with a uniform boundary temperature. In this work, we examine Reynolds number in the range of 10^2–10^3 and particle volume fraction in the range of 1–2%. Five different amplitudes of the wavy channel are tested. The pressure and velocity decoupling are handled with a SIMPLE algorithm and the equations are discretized using the FVM. The validation is carried out for the flow of nanofluid inside a horizontal tube [39] against experimental [40] and theoretical studies [41].

2. Materials and Methods

CFD analysis of an asymmetric wavy channel is investigated. The computational domain of the analyzed channel is a single periodic unit of height, 2H, and foot length, L. The wavy profile is given as

$$y = A\,cos(2\pi x/\lambda_o) \quad (1)$$

where A and λ_o are the amplitude and length of the wave. Here, five-wave amplitudes are considered as shown in Figure 1a; the base case wavy channel amplitude is given by A2, whereas A1, A3, A4, and A5 are scaled from A2 by incrementing the amplitude by 125%, 75%, 50%, and 25%, respectively.

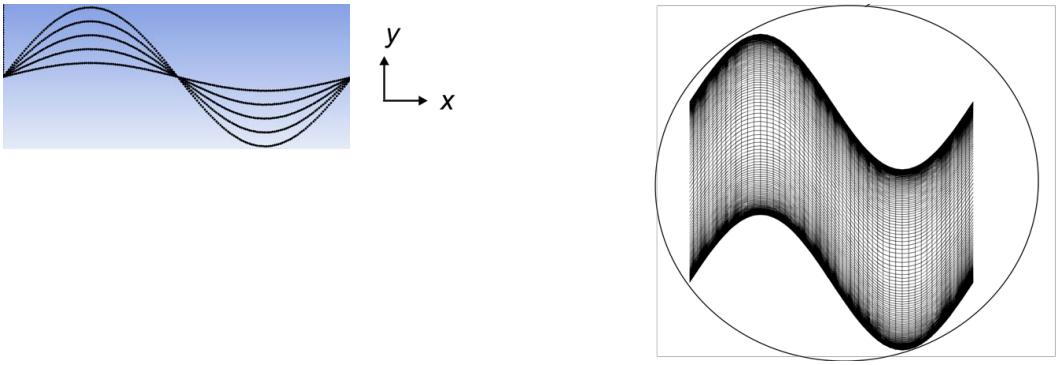

(**a**) (**b**)

Figure 1. Wavy profile and a computational domain: (**a**) The wave profile, showing various amplitudes; (**b**) The geometry used for the computational domain channel foot length, sample mesh of a periodic unit.

Various inflow rates are considered in the ranges of the laminar regime, Reynolds number 10^2–10^3; and the working fluid is water Al_2O_3–Cu/water hybrid nanofluid with constant properties.

The number of meshes with increasing sizes, (40 × 20), (64 × 34) and (102 × 54) are tested to determine an optimal mesh size. The refinement effect on the average Nusselt number and friction factor is within 2%. A non-uniform, quad-mapped mesh consisting of 5400 elements is adequate for all computations.

Physical properties of nanofluids including the effective density and specific heat are evaluated using the classical mixture formula as follows [42,43].

Density:

$$\rho_{hnf} = \rho_f\left(1 - \varphi_{hnp}\right) + \rho_{Al_2O_3}\,\varphi_{Al_2O_3} + \rho_{Cu}\,\varphi_{Cu} \tag{2}$$

Specific heat:

$$(\rho c_P)_{\mathrm{hnf}} = \left(1 - \varphi_{\mathrm{hnp}}\right)(\rho c_P)_{\mathrm{f}} + (\rho c_P)_{Al_2O_3}\,\varphi_{Al_2O_3} + (\rho c_P)_{\mathrm{Cu}}\,\varphi_{\mathrm{Cu}} \tag{3}$$

where $\varphi_{\mathrm{hnp}} = \varphi_{Al_2O_3} + \varphi_{\mathrm{Cu}}$

Since the volume fraction considered here is less than 10%, the fluid mixture is considered a Newtonian fluid. The viscosity and thermal conductivity are given as [44].

Dynamic viscosity:

$$\mu_{nf} = \mu_{bf}\left(123\,\varphi^2 + 7.3\,\varphi + 1\right) \tag{4}$$

Thermal conductivity:

$$k_{nf} = k_{bf}\left(4.97\,\varphi^2 + 2.72\,\varphi + 1\right) \tag{5}$$

It has been discussed by Chamkha et al. [45] and Mehryan et al. [46] that when considering the thermal conductivity of the Al_2O_3–Cu/water hybrid nanofluid, either the Levin and Miller [47] or Bruggman [48] are commonly used. Lundgren [49], Brinkman [50], or Batchelor [51] models are employed in the determination of viscosity of the Al_2O_3–Cu/water hybrid nanofluid. It is interesting to note that at a volume fraction of 2%, the values of conductivity and viscosity models deviate from the experimental results [52] by as much as 6% and 90%, respectively. Therefore, in this study and following the studies [45,52], the experimentally determined values of the conductivity and viscosity of the hybrid nanofluid should be utilized. The nanofluid properties are obtained using the above equations as given by [28] and summarized in Table 1.

Table 1. Properties of considered nanofluids, single-phase model. For the nanofluid [28] and hybrid nanofluid Cu–Al2O3 [45].

φ		ρ (kg/m^3)	c_p (J/kg K)	μ (Pa s)	k (W/m K)
0.00	Water	998.2	4182	998×10^{-6}	0.597
0.01	Al_2O_3	1027.9	4050	1080×10^{-6}	0.614
0.02	Al_2O_3	1057.6	3925	1190×10^{-6}	0.631
0.01	Cu–Al_2O_3	1029.8	4076	1602×10^{-6}	0.657
0.02	Cu–Al_2O_3	1061.4	3976	1935×10^{-6}	0.685

It is supposed that the flow is steady and periodically fully developed hydrodynamically and thermally. The governing equations of continuity, momentum, and energy for the fluid flow and heat transfer in the periodic domain are as follows:

Continuity:

$$\frac{\partial u}{\partial x} + \frac{\partial v}{\partial y} = 0 \tag{6}$$

x-direction conservation of momentum:

$$\rho_{hnf}\left(u\frac{\partial u}{\partial x} + v\frac{\partial u}{\partial y}\right) = \beta - \frac{\partial P}{\partial x} + \mu_{hnf}\left(\frac{\partial^2 v}{\partial x^2} + \frac{\partial^2 v}{\partial y^2}\right) \tag{7}$$

y-direction conservation of momentum:

$$\rho_{hnf}\left(u\frac{\partial v}{\partial x} + v\frac{\partial v}{\partial y}\right) = -\frac{\partial P}{\partial y} + \mu_{hnf}\left(\frac{\partial^2 v}{\partial x^2} + \frac{\partial^2 v}{\partial y^2}\right) \tag{8}$$

The energy equation:

$$(\rho c_P)_{hnf}\left(u\frac{\partial T}{\partial x} + v\frac{\partial T)}{\partial y}\right) = k_{hnf}\left(\frac{\partial^2 T}{\partial x^2} + \frac{\partial^2 T}{\partial y^2}\right) \tag{9}$$

The upstream and downstream ends of the solution domain are subjected to the periodicity conditions [53,54], given as:

$$u(0, y) = u(L, y) \tag{10}$$

$$v(0, y) = v(L, y) \tag{11}$$

$$P(0, y) = P(L, y) \tag{12}$$

$$\frac{T(0, y) - T_w}{T_b(0) - T_w} = \frac{T(L, y) - T_w}{T_b(L) - T_w} \tag{13}$$

The boundary conditions at the solid surface are provided by the no-slip requirement, and the thermal boundary condition employed here is a uniform wall temperature. The Reynolds number and friction factor are defined as

$$Re = \rho\, \overline{u} D_H / \mu \tag{14}$$

$$f = \beta\, D_H / \left(\frac{1}{2}\rho \overline{u}^2\right) \tag{15}$$

where

$$\overline{u} = \frac{1}{H}\int_0^H u dy \tag{16}$$

$$D_H = 2H \tag{17}$$

The dimensionless temperature θ is defined by

$$\theta = \frac{T - T_w}{T_b - T_w} \tag{18}$$

where the bulk temperature is given by

$$T_b = \int_0^H |u| T dy / \int_0^H |u| dy \tag{19}$$

The average Nusselt number is defined as

$$\overline{Nu} = \overline{h}\, D_H / k \tag{20}$$

where the heat transfer coefficient is given as

$$\overline{h} = Q / 2L_S\, LMTD \tag{21}$$

Q is the rate of heat transfer over the periodic module. Ls represents the heated surface area of the channel, and the log-mean temperature difference (LMTD) is defined as

$$LMTD = \frac{[T_w - T_b(L)] - [T_w - T_b(0)]}{\ln\{[T_w - T_b(L)] / [T_w - T_b(0)]\}} \tag{22}$$

The local heat transfer coefficient over the channel surface is given by

$$h = q / (T_w - T_b) \tag{23}$$

where q is the local heat flux.

The governing equations in terms of primitive variables along with the cyclic boundary conditions Equations (6)–(13) are solved using the Finite Volume Method (FVM). The computational domain consists of a periodic segment as specified by Equation (1). The convection-diffusion was handled using the upwind scheme, while the SIMPLE algorithm [31] was employed to decouple the pressure and velocity. Nanofluid Al_2O_3 and hybrid nanofluid Cu–Al_2O_3 with a concentration of 1% and 2% are used as the working fluid and compared to pure water. The Reynolds number range was between 10^2 and 10^3. The solutions are deemed converged when the residuals of the mass conservation and velocity fall below 10^{-5} and the energy residuals are less than 10^{-8}. Experimental data on nanofluids flowing inside a wavy channel are lacking. However, the accuracy of the computational method has been validated for a circular tube against the numerical and experimental data of [39] for Al_2O_3/water nanofluid flow inside a circular tube of 12.4 mm in diameter, ϕ = 1% and dp = 30 nm using the Dirichlet thermal boundary condition. The enhancement in the average heat transfer, h_r, was validated for the Reynolds number in the laminar range. It is shown in Figure 2 that generally excellent agreement is found with the computational model and good agreement with the experimental results.

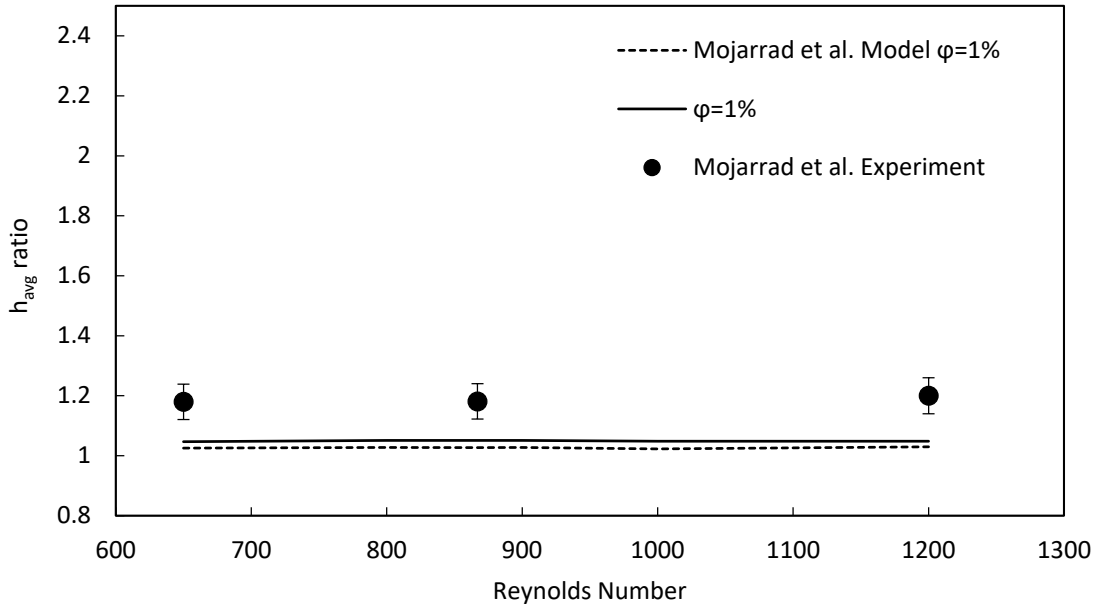

Figure 2. Model for nanofluid inside a horizontal tube subject to a uniform wall temperature with work presented by [39,40].

3. Results

This section highlights the results of the conducted numerical experiments to show the effect of using hybrid nanofluid in a wavy channel. We study the influence of changing the nanoparticles volume fraction in the base fluid, the varying amplitude of the channel, and the effect of Reynolds number on the thermal performance. We maintained a constant wave footprint length for the spatially periodic module as shown in Figure 1a.

The non-dimension local wall shear stress distributions (WSS) are shown for the top surface with amplitude A2 (Figure 3a) and amplitude A4 (Figure 3b).

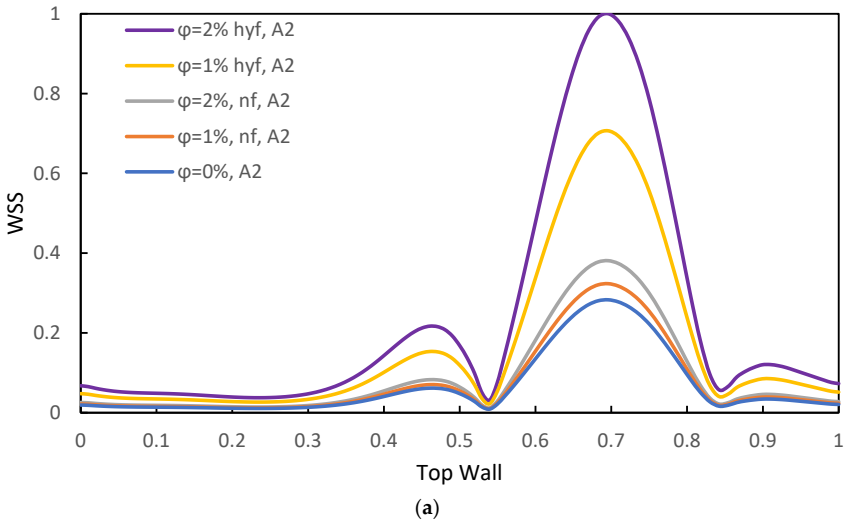

(**a**)

Figure 3. *Cont.*

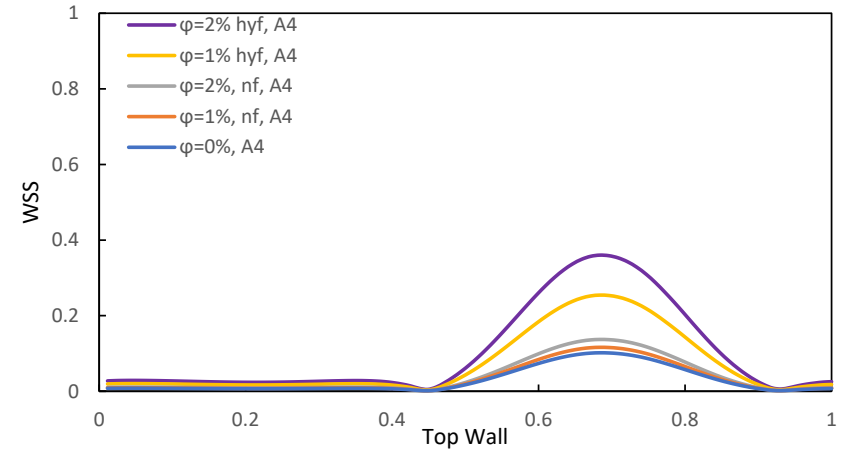

(**b**)

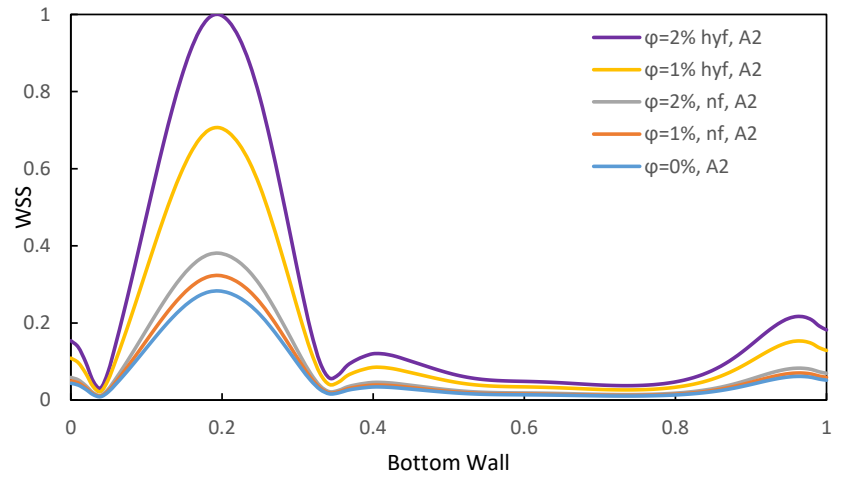

(**c**)

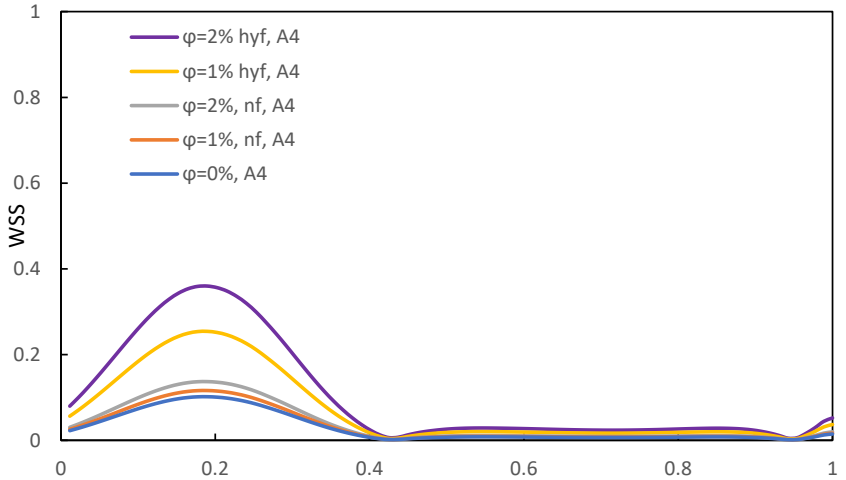

(**d**)

Figure 3. Local wall shear stress (Pa s), Re = 300. Top wall: (**a**) Amplitude A2; (**b**) Amplitude A4. Bottom wall: (**c**) Amplitude A2; (**d**) Amplitude A4.

For nanoparticle volume fraction φ = 2%, doubling the wave amplitude (Figure 3a,b) increases the peak local shear by a factor of 2.5, this is because of increased losses in the expanding recirculating fluid zones of the curved regions of the channel. On the other hand, for a fixed amplitude A2, i.e., Figure 3a,

increasing the nanoparticle concentration from φ = 1% to φ = 2% increases the peak of the local shear stress by a factor of 1.5, which is directly related to the increase in the effective fluid viscosity with increasing nanoparticle volume fraction. Figure 3c,d shows similar trends of the local shear stress at the bottom channel surface, where the location of the peak is shifted due to the asymmetry of the channel configuration.

Figure 4a explains the pressure gradient required to drive the flow through the periodic module. We note a significant increase with greater amplitudes and larger volume fractions for both nanofluid and hybrid nanofluid. The hybrid nanofluid increases the pressure gradient requirement by as much as 3.5-fold in comparison to the nanofluid. This is due to the increased resistance with the growing recirculating fluid zones and the higher viscosity of hybrid nanofluid in contrast to the nanofluid. Another way to examine this effect is by studying the friction factor results for various amplitudes at 1% and 2% nanoparticle volume fractions as depicted in Figure 4b.

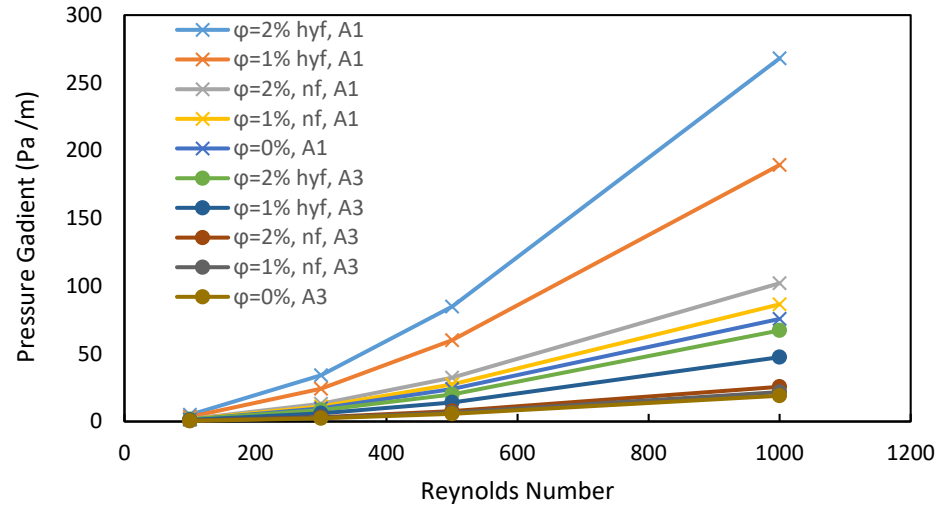

(**a**)

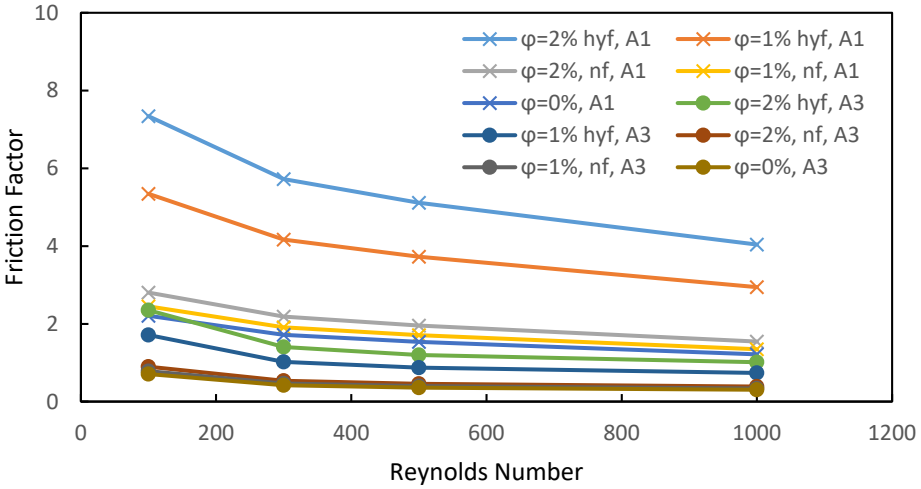

(**b**)

Figure 4. (**a**) Pressure gradient. (**b**) Friction factor.

Figure 5a,b shows the local convective heat transfer coefficient in terms of Nusselt number at the channel top surface. Clearly, a two-fold increase in the amplitude results in a factor of 1.7 increase

in the peak heat transfer coefficient. At a fixed amplitude i.e., A2, and particle concentration of 1%, a significant increase in heat transfer of nearly 14% is noticed when hybrid nanofluid is utilized in comparison to a marginal increase for the case of nanofluid. A less pronounced increase of 3% in the peak heat transfer coefficient is due to the presence of 2% volume fraction nanoparticles in the base fluid in contrast to 1%. This change can be attributed to the improved thermal conductivity with the addition of nanoparticles. Figure 5c,d shows the local heat transfer coefficient at the channel bottom surface. The improvement in the heat transfer is similar to the channel top surface, and the shift in the location of the peak is attributed to the asymmetry of the channel. Moreover, Figure 5c,d shows the effect of changing Reynolds number from 500 to 300 while having the same wave amplitude. This results in decreasing the Nusselt number by nearly 20%.

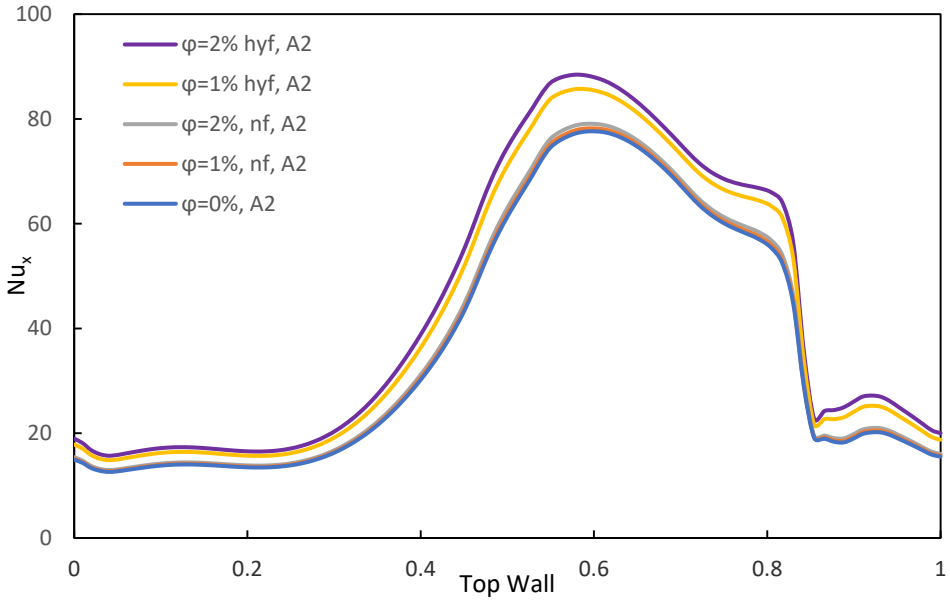

(**a**)

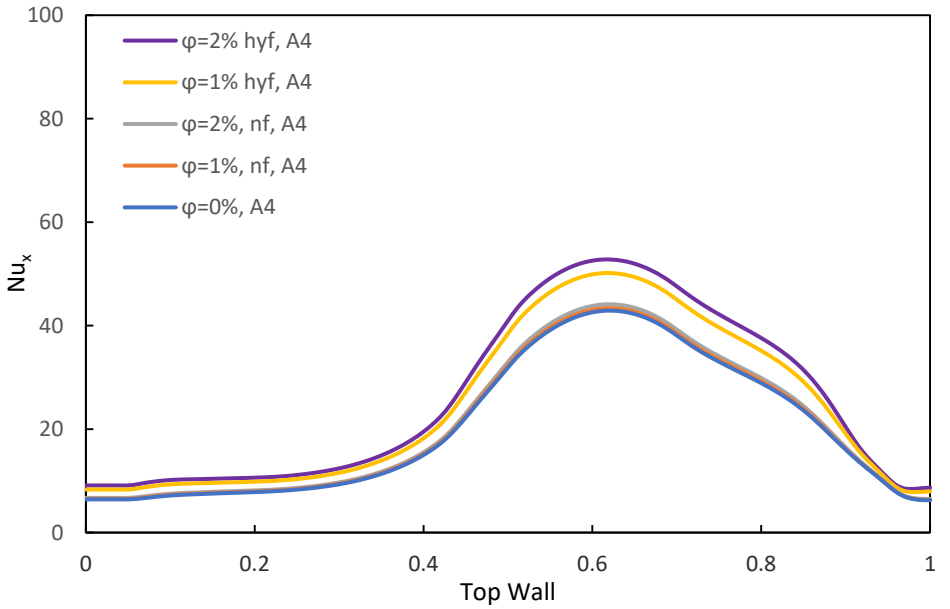

(**b**)

Figure 5. *Cont.*

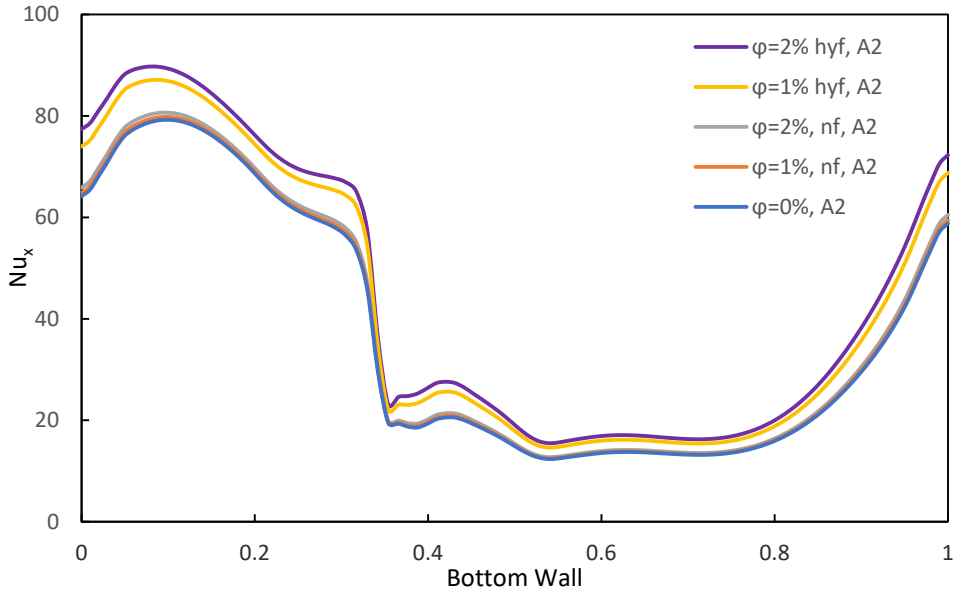

(**c**)

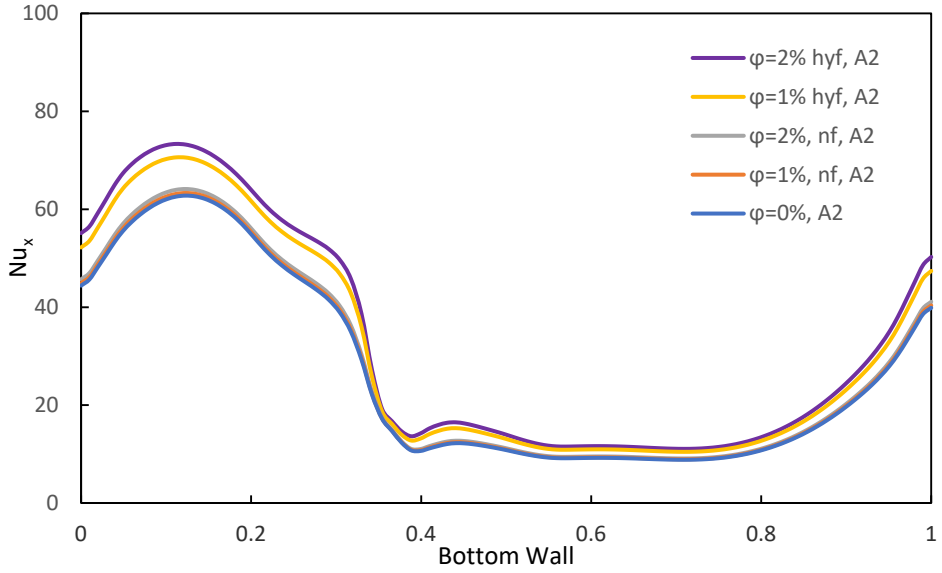

(**d**)

Figure 5. Local Nusselt number, top wall, Re = 500: (**a**) Amplitude A2; (**b**) Amplitude A4. Bottom wall, amplitude A2: (**c**) Re = 500; (**d**) Re = 300.

Figure 6 illustrates the geometric effect, the nanoparticle composition (Al_2O_3 vs. $Cu–Al_2O_3$) and the inertial influence on the dimensionless heat transfer or the Nusselt number. We observe that the average Nusselt number is increased by 25% when the channel amplitude is doubled due to increased advection effect driven by vigorous mixing in an expanded recirculating fluid zone. A 2% hybrid nanoparticles addition to the base fluid results in even greater enhancement in the heat transfer by as much as 46%; this increase is directly related to the increase in fluid conductivity. The enhancement of heat transfer with increased waviness happens at the cost of additional frictional effects.

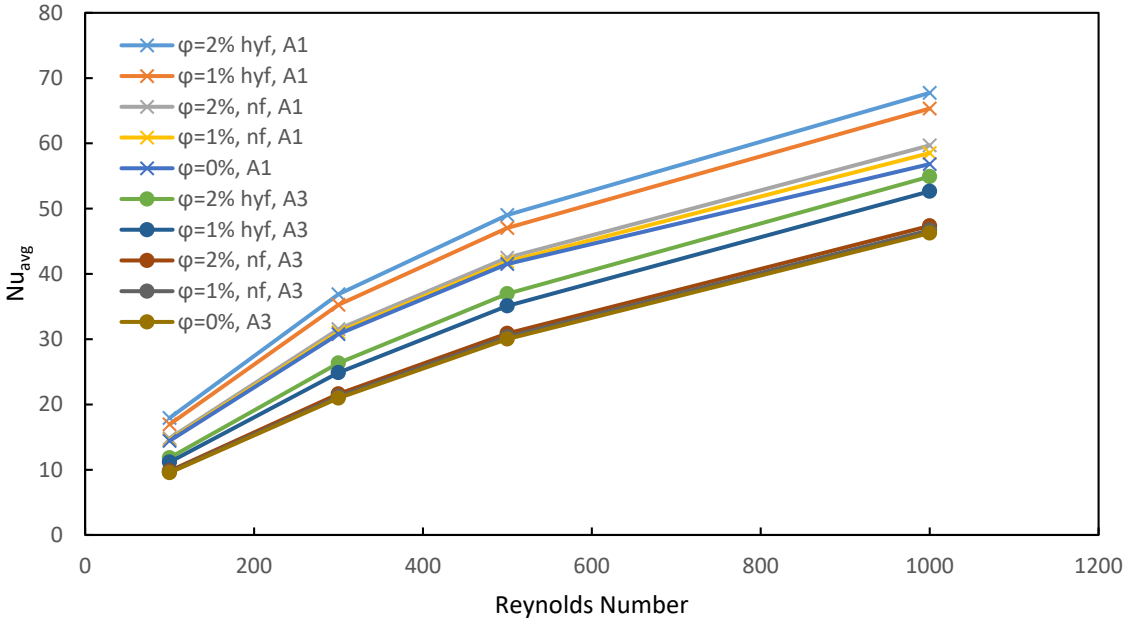

Figure 6. Average Nusselt number, bottom wall, Amplitude A1 and A3.

4. Discussion

The average Nusselt number and the friction factor are correlated to Reynolds number and other parameters as follows:

$$Nu = C_1\left(\frac{A}{\lambda_o}\right)^{n_1}\varphi^{m_1}Re^{s_1} \tag{24}$$

$$f = C_2\left(\frac{A}{\lambda_o}\right)^{n_2}\varphi^{m_2}Re^{s_2} \tag{25}$$

where the constant C_1, C_2, n_1, n_2, m_1, m_2, s_1, s_2 for the case of nanofluid and hybrid nanofluid are given in Table 2.

Table 2. Correlations for nanofluid and hybrid nanofluid.

	H_2O–Al_2O_3 *Nu* (Equation (24))	H_2O–Al_2O_3 *f* (Equation (25))	H_2O–Cu–Al_2O_3 *Nu* (Equation (24))	H_2O–Cu–Al_2O_3 *f* (Equation (25))
C1	2.787		3.9	
C2		614.003		4238.649
n1	0.697		0.697	
n2		1.643		1.643
m1	0.0232		0.0232	
m2		0.198		0.198
s1	0.631		0.631	
s2		−0.433		−0.433
R^2	0.992	0.932	0.992	0.933

The above correlations are valid for $\varphi > 0$, where A and λ_0 are the amplitude and length of the wave. The R^2 values for correlations (24) and (25) are 0.992 and 0.933 for the nanofluid case while these values are 0.992 and 0.932, respectively for the hybrid nanofluid. The expected average error for either correlation is less than 1%.

In summary, increasing the wave amplitude results in enhancing the local and average heat transfer due to increased mixing in the vicinity of the curved segments of the top and bottom channel

surfaces. It is also observed that as Reynolds number increases, the increasing inertial effect intensifies the recirculation zones even more, resulting in its growth. Moreover, it increases the thermal transport exchange between these zones and the fluid in the core region of the channel. In addition, the presence of the hybrid nanoparticles effectiveness in heat transfer enhancement can be attributed to the increase in the thermal conductivity of the base fluid. However, the augmentation of heat transfer with increased waviness and nanoparticle concentration takes place at the cost of increased frictional losses.

5. Conclusions

A steady two-dimensional analysis of a periodically fully developed flow through a wavy channel module has been carried out. It is found that increasing the volume fraction of nanoparticles increases both the heat transfer rate and frictional effects. The increase in heat transfer is marginal with nanoparticle φ = 1% and 2%, and corresponds to an increase of the Nusselt number of 1% and 3%. However, the addition of hybrid nanoparticle has a significant impact with an increase of 16% and 22% in the Nusselt number with the addition of 1% and 2% volume fraction. This is realized at the cost of increasing the friction factor by 1.34 and 2.33-fold for the Cu–Al_2O_3 fluid volume fraction of 1% and 2% respectively. This is in contrast to a moderate increase of 11% and 27% for the similar volume fractions of Al_2O_3 nanoparticles. In addition, the increase in the channel wave amplitude by 25% enhances the heat transfer by nearly 12% at the cost of an increase of 15% in frictional losses.

Author Contributions: A.A. carried out the computational simulations. W.A.-K. generated the proposed correlations. W.K. prepared the state of art on the topic. All authors have read and agreed to the published version of the manuscript.

Funding: This research received no external funding.

Conflicts of Interest: The authors declare no conflict of interest.

References

1. Hussien, A.A.; Al-Kouz, W.; Yusop, N.M.; Abdullah, M.Z.; Janvekar, A.A. A Brief Survey of Preparation and Heat Transfer Enhancement of Hybrid Nanofluids. *Stroj. Vestn. J. Mech. Eng.* **2019**, *65*, 441–453. [CrossRef]
2. Gawande, V.; Ramgadia, A.; Saha, A. Numerical study of flow and heat transfer in wavy channel. In Proceedings of the 20th National and 9th International ISHMT-ASME Heat and Mass Transfer Conference, Mumbai, India, 4–6 January 2010.
3. Ramgadia, A.G.; Saha, A.K. Fully developed flow and heat transfer characteristics in a wavy passage: Effect of amplitude of waviness and Reynolds number. *Int. J. Heat Mass Transf.* **2012**, *55*, 2494–2509. [CrossRef]
4. Niceno, B.; Nobile, E. Numerical analysis of fluid flow and heat transfer in periodic wavy channels. *Int. J. Heat Fluid Flow* **2001**, *22*, 156–167. [CrossRef]
5. Ramgadia, A.G.; Saha, A.K. Numerical study of fully developed flow and heat transfer in a wavy passage. *Int. J. Therm. Sci.* **2013**, *67*, 152–166. [CrossRef]
6. Hossain, M.Z.; Islam, A.K.M.S. Fully developed flow structures and heat transfer in sine-shaped wavy channels. *Int. Commun. Heat Mass Transf.* **2004**, *31*, 887–896. [CrossRef]
7. Hossain, M.Z.; Islam, A.K.M.S. Numerical investigation of fluid flow and heat transfer characteristics in Sine, Triangular, and Arc-shaped channels. *Therm. Sci.* **2007**, *11*, 17–26. [CrossRef]
8. Stone, K.; Vanka, S.P. Numerical study of Developing Flow and Heat transfer in a wavy passage. *J. Fluids Eng.* **1999**, *121*, 713–719. [CrossRef]
9. Sarkar, M.; Paramane, S.B.; Sharma, A. Periodically Fully Developed Heat and Fluid Flow Characteristics in a Furrowed Wavy Channel. *Heat Transf. Eng.* **2016**, *38*, 278–288. [CrossRef]
10. Bahaidarah, H.M.S.; Anand, N.K.; Chen, H.C. Numerical study of heat and momentum transfer in channels with wavy walls. *Numer. Heat Transf. A* **2005**, *47*, 417–439. [CrossRef]
11. Bahaidarah, H.M.; Anand, N.K.; Chen, H.C. Numerical Study of Fluid Flow and Heat Transfer over a Bank of Flat Tubes. *Numer. Heat Transf. A* **2005**, *48*, 359–385. [CrossRef]
12. Bahaidarah, H.M.S. A numerical study of Fluid flow and Heat transfer characteristics in channels with staggered wavy walls. *Numer. Heat Transf. A* **2007**, *51*, 877–898. [CrossRef]

13. Xie, G.N.; Wang, Q.W.; Zeng, M.; Luo, L.Q. Numerical investigation of heat transfer and fluid flow characteristics inside a wavy channel. *Heat Mass Transf.* **2007**, *43*, 603–611. [CrossRef]
14. Rush, T.A.; Newell, T.A.; Jacobi, A.M. An experimental study of Flow and Heat transfer in sinusoidal wavy passage. *Int. J. Heat Mass Transf.* **1998**, *42*, 1541–1553. [CrossRef]
15. Nishimura, T.; Murakami, S.; Arakawa, S.; Kawamura, Y. Flow observations, and mass transfer characteristics in symmetrical wavy-walled channels at moderate Reynolds number for steady flow. *Int. J. Heat Mass Transf.* **1990**, *33*, 835–845.
16. Nishimura, T.; Ohori, Y.; Kawamura, Y. Flow characteristics in a channel with symmetric wavy wall for steady flow. *J. Chem. Eng. Jpn.* **1984**, *17*, 466–471. [CrossRef]
17. Nishimura, T.; Ohori, Y.; Kajimoto, Y.; Kawamura, Y. Mass Transfer Characteristics in a Channel with Symmetric Wavy Wall for Steady Flow. *J. Chem. Eng. Jpn.* **1985**, *18*, 550–555. [CrossRef]
18. Nishimura, T.; Kajimoto, Y.; Kawamura, Y. Mass Transfer Enhancement in Channels with Symmetric Wavy Wall. *J. Chem. Eng. Jpn.* **1986**, *19*, 142–144. [CrossRef]
19. Nishimura, T.; Yano, K.; Yoshino, T.; Kawamura, Y. Occurrence, and Structure of Taylor-Goertler Vortices Induced in Two-Dimensional Wavy Channels for Steady Flow. *J. Chem. Eng. Jpn.* **1990**, *23*, 697–703. [CrossRef]
20. Nishimura, T.; Bian, Y.N.; Matsumoto, Y.; Kunitsugu, K. Fluid flow and mass transfer characteristics in a sinusoidal wavy-walled tube at moderate Reynolds numbers for steady flow. *Heat Mass Transf.* **2003**, *39*, 239–248. [CrossRef]
21. Stone, K.; Vannka, S.P. *Review of Literature on Heat Transfer Enhancement in Compact Heat Exchangers*; Air Conditioning and Refrigeration Center, University of Illinois: Urbana, IL, USA, 1996.
22. Choi, U.S. Enhancing thermal conductivity of fluids with nanoparticles. *ASME Fluids Eng. Div.* **1995**, *231*, 99–103.
23. Xuan, Y.; Li, Q. Heat transfer enhancement of nanofluids. *Int. J. Heat Fluid Flow* **2000**, *21*, 58–64. [CrossRef]
24. Vajjha, R.S.; Das, D.K. Experimental determination of thermal conductivity of three nanofluids and development of new correlations. *Int. J. Heat Mass Transf.* **2009**, *52*, 4675–4682. [CrossRef]
25. Zerinc, S.O.; Kakac, S.; Yazicioglu, A.G. Enhanced thermal conductivity of nanofluids: A state-of-the-art review. *Microfluid. Nanofluid.* **2010**, *8*, 145–170. [CrossRef]
26. Khedkar, R.S.; Sonawane, S.S.; Wasewa, K.L. Influence of CuO nanoparticles in enhancing the thermal conductivity of water and mono ethylene glycol-based nanofluids. *Int. Commun. Heat Mass Transf.* **2012**, *39*, 665–669. [CrossRef]
27. Khanafer, K.; Vafai, K. A critical synthesis of thermophysical characteristics of nanofluids. *Int. J. Heat Mass Transf.* **2011**, *54*, 4410–4428. [CrossRef]
28. Shafahi, M.; Bianco, M.; Vafai, K.; Manca, O. Thermal performance of flat-shaped heat pipes using nanofluids. *Int. J. Heat Mass Transf.* **2010**, *53*, 1438–1445. [CrossRef]
29. Liu, Z.H.; Li, Y.Y.; Bao, R. Compositive effect of nanoparticle parameter on thermal performance of cylindrical micro-grooved heat pipe using nanofluids. *Int. J. Therm. Sci.* **2011**, *50*, 558–568. [CrossRef]
30. Alizad, K.; Vafai, K.; Shafahi, M. Thermal performance and operational attributes of the startup characteristics of flat-shaped heat pipes using nanofluids. *Int. J. Heat Mass Transf.* **2012**, *55*, 140–155. [CrossRef]
31. Yang, Y.T.; Wang, Y.H.; Tseng, P.K. Numerical optimization of heat transfer enhancement in a wavy channel using nanofluids. *Int. J. Heat Mass Transf.* **2013**, *51*, 9–17. [CrossRef]
32. Rashidi, M.M.; Hosseini, A.; Pop, I.; Kumar, S.; Freidoonimehr, N. Comparative numerical study of single and two-phase models of nanofluid heat transfer in wavy channel. *Appl. Math. Mech.* **2014**, *35*, 831–848. [CrossRef]
33. Akdag, U.; Akcay, S.; Demiral, D. Heat transfer enhancement with laminar pulsating nanofluid flow in a wavy channel. *Int. J. Heat Mass Transf.* **2014**, *59*, 17–23. [CrossRef]
34. Shehzad, N.; Zeeshan, A.; Ellahi, R.; Vafai, K. Convective heat transfer of nanofluid in a wavy channel: Buongiorno's mathematical model. *J. Mol. Liq.* **2016**, *222*, 446–455. [CrossRef]
35. Albojamal, A.; Hamzah, H.; Haghighi, A.; Vafai, K. Analysis of nanofluid transport through a wavy channel. *Numer. Heat Transf. Part A Appl.* **2017**, *72*, 869–890. [CrossRef]
36. Ahmed, M.A.; Shuaib, N.H.; Yusoff, M.Z. Numerical investigations on the heat transfer enhancement in a wavy channel using nanofluid. *Int. J. Heat Mass Transf.* **2012**, *55*, 5891–5898. [CrossRef]

37. Hader, M.; Al-Kouz, W. Performance of a hybrid photovoltaic/thermal system utilizing water-Al_2O_3 nanofluid and fins. *Int. J. Energy Res.* **2018**, *43*, 219–230. [CrossRef]
38. Bozorg, M.; Doranehgard, M.; Hong, K.; Xiong, Q. CFD study of heat transfer and fluid flow in a parabolic trough solar receiver with internal annular porous structure and synthetic oil-Al_2O_3 nanofluid. *Renew. Energy* **2020**, *145*, 2598–2614. [CrossRef]
39. Mojarrad, M.S.; Keshavarz, A.; Shokouhi, A. Nanofluids thermal behavior analysis using a new dispersion model along with single-phase. *Heat Mass Transf.* **2013**, *49*, 1333–1343. [CrossRef]
40. Heris, S.Z.; Esfahany, M.N.; Etemad, G. Numerical investigation of nanofluid laminar convective heat transfer through a circular tube. *Numer. Heat Transf. Part A Appl.* **2007**, *52*, 1043–1058. [CrossRef]
41. Nasrin, R.; Alim, M. Free convective flow of nanofluid having two nanoparticles inside a complicated cavity. *Int. J. Heat Mass Transf.* **2013**, *63*, 191–198. [CrossRef]
42. Maïga, S.E.B.; Nguyen, C.T.; Galanis, N.; Roy, G.; Maré, T.; Coqueux, M. Heat transfer enhancement in turbulent tube flow using Al_2O_3 nanoparticle suspension. *Int. J. Num. Methods Heat Fluid Flow* **2006**, *16*, 275–292. [CrossRef]
43. Pak, B.C.; Cho, Y.I. Hydrodynamic and heat transfer study of dispersed fluids with submicron metallic oxide particles. *Exp. Heat Transf.* **1998**, *11*, 151–170. [CrossRef]
44. Maïga, S.E.B.; Palm, S.J.; Nguyen, C.T.; Roy, G.; Galanis, N. Heat transfer enhancement by using nanofluids in forced convection flows. *Int. J. Heat Fluid Flow* **2005**, *26*, 530–546. [CrossRef]
45. Chamkha, A.J.; Sazegar, S.; Jamesahar, E.; Ghalabaz, M. Thermal non-equilibrium heat transfer modeling of hybrid nanofluids in a structure composed of layers of solid and porous media and free nanofluids. *Energies* **2019**, *12*, 541. [CrossRef]
46. Mehryan, S.A.; Izadapanahi, E.; Ghalambaz, M.; Chamkha, A.J. Mixed convection flow caused by an oscillating cylinder in a square cavity filled with Cu-Al_2O_3/water, hybrid nanofluid. *J. Therm. Anal. Calorim.* **2019**, *137*, 965–982. [CrossRef]
47. Levin, M.L.; Miller, M.A. Maxwell's "Treatise on Electricity and Magnetism". *Sov. Phys. Uspekhi* **1981**, *24*, 904. [CrossRef]
48. Brüggemann, V.D. Berechnung verschiedener physikalischer Konstanten von heterogenen Substanzen. I. Dielektrizitätskonstanten und Leitfähigkeiten der Mischkörper aus isotropen Substanzen. *Ann. Phys.* **1935**, *416*, 636–664. [CrossRef]
49. Lundgren, T.S. Slow flow through stationary random beds and suspensions of spheres. *J. Fluid Mech.* **1972**, *51*, 273–299. [CrossRef]
50. Brinkman, H.C. The viscosity of concentrated suspensions and solutions. *J. Chem. Phys.* **1952**, *20*, 571. [CrossRef]
51. Batchelor, G.K. The effect of Brownian motion on the bulk stress in a suspension of spherical particles. *J. Fluid Mech.* **1977**, *83*, 97–117. [CrossRef]
52. Suresh, S.; Venkitaraj, K.P.; Selvakumar, P.; Chandrasekar, M. Synthesis of Al_2O_3–Cu/water hybrid nanofluids using two-step method and its thermophysical properties. *Colloids Surf. A* **2011**, *388*, 41–48. [CrossRef]
53. Alshare, A.A.; Simon, T.W.; Strykowski, P.J. International Journal of Heat and Mass Transfer Simulations of flow and heat transfer in a serpentine heat exchanger having dispersed resistance with porous-continuum and continuum models. *Int. J. Heat Mass Transf.* **2010**, *53*, 1088–1099. [CrossRef]
54. Patankar, S.V.; Liu, C.H.; Sparrow, E.M. Fully Developed Flow and Heat Transfer in Ducts Having Streamwise-Periodic Variations of Cross-Sectional Area. *J. Heat Transf.* **1977**, *99*, 180. [CrossRef]